

norbornyl polycarbonate ($T_{1\rho}(C)$) (in comparisons with tetrachloro polycarbonate and other polymers with a similar $H_1(C)$ dependence) are not in line with its low impact strength. This demonstrates that the correlation between a single average $T_{1\rho}(C)$ value and impact strength is, in fact, not universal and that for some systems a more elaborate use of $T_{1\rho}(C)$ relaxation behavior may produce a better guide to deformation events on a molecular scale.

In summary, the extensive collection of relaxation data discussed in the previous three sections supports a general connection between the macroscopic physical property of toughness and microscopic molecular motion for polycarbonate and various modifications of polycarbonate but also defines a number of exceptions and qualifications (mostly dealing with sample geometry) which necessarily limit the utility of this connection in practical applications.

References and Notes

- (1) J. Schaefer, E. O. Stejskal, T. R. Steger, M. D. Sefcik, and R. A. McKay, *Macromolecules*, preceding paper in this issue.
- (2) T. T. P. Cheung and R. Yaris, *J. Chem. Phys.*, **72**, 3604 (1980).
- (3) J. Schaefer, E. O. Stejskal, and R. Buchdahl, *Macromolecules*, **10**, 384 (1977).
- (4) E. O. Stejskal and J. Schaefer, *J. Magn. Reson.*, **14**, 160 (1974).
- (5) E. O. Stejskal and J. Schaefer, *J. Magn. Reson.*, **18**, 560 (1975).
- (6) V. R. Cross, R. K. Hester, and J. S. Waugh, *Rev. Sci. Instrum.*, **47**, 1486 (1976).
- (7) E. R. Andrew, A. Bradbury, and R. G. Eades, *Nature (London)*, **182**, 1569 (1958).
- (8) A. Pines, M. G. Gibby, and J. S. Waugh, *J. Chem. Phys.*, **59**, 569 (1973).
- (9) T. R. Steger, SPE Proceedings of the National Technical Conference, Nov 1979, p 89.
- (10) J. Schaefer and E. O. Stejskal, *Top. Carbon-13 NMR Spectrosc.*, **3**, 319 (1979).
- (11) G. Allen, D. C. W. Morley, and T. Williams, *J. Mater. Sci.*, **8**, 1449 (1973).
- (12) J. Schaefer, *Macromolecules*, **8**, 882 (1973).
- (13) See, for example, S. Sternstein in "Polymeric Materials", American Society for Metals, Metals Park, OH, 1975, p 369.
- (14) R. F. Boyer, *Polym. Eng. Sci.*, **8**, 161 (1968).
- (15) L. J. Broutman and S. M. Krishnakumar, *Polym. Eng. Sci.*, **16**, 74 (1976).
- (16) M. Parvin and J. G. Williams, *Int. J. Frac.*, **11**, 963 (1975).
- (17) R. J. Morgan and J. E. O'Neal, *J. Polym. Sci., Polym. Phys. Ed.*, **14**, 1053 (1976).
- (18) N. J. Mills, *J. Mater. Sci.*, **11**, 363 (1976).
- (19) D. L. Watts and E. P. Perry, *Polymer*, **19**, 248 (1978).
- (20) S. E. B. Petrie, R. S. Moore, and J. R. Flick, *J. Appl. Phys.*, **43**, 4318 (1972).
- (21) W. J. Jackson and J. R. Caldwell, *J. Appl. Polym. Sci.*, **11**, 227 (1967).

Analysis of the Room-Temperature Molecular Motions of Poly(ethylene terephthalate)

M. D. Sefcik, Jacob Schaefer,* E. O. Stejskal, and R. A. McKay

Monsanto Company, Corporate Research Laboratories, St. Louis, Missouri 63166.

Received December 3, 1979

ABSTRACT: Carbon-13 rotating-frame relaxation parameters have been obtained from magic-angle high-resolution ^{13}C NMR spectra of various poly(ethylene terephthalates). Comparisons of $\langle T_{1\rho}(C) \rangle$'s and $\langle T_{1S}(\text{ADRF}) \rangle$'s show that $T_{1\rho}(C)$ relaxation is a spin-lattice process for the amorphous material and so can be used to characterize molecular motion in the low-to-mid-kilohertz frequency range. Annealing below T_g reduces the mid-kilohertz rotational segmental motions of the ethylene groups in poly(ethylene terephthalate). The transition from ductile to brittle mechanical failure observed with low-temperature annealing may result from the loss of these cooperative components of main-chain motion. By contrast, either the amplitude of the mid-kilohertz phenyl motions increases or the frequency decreases during this period, consistent with the notion that precrystalline organization leads to coplanarity of the phenyl rings, an increase in the carbonyl-phenyl dihedral angle, and a reduction of the barrier to internal phenyl-group rotation. Annealing above T_g allows conformations at the ethylene linkages to change from gauche to trans. On the basis of a resolution of the ethylene-carbon resonance into contributions from gauche and trans conformations, a reduction in molecular motion is observed for ethylene groups with gauche conformations in the amorphous region after annealing above T_g , while the dynamic behavior of the trans-ethylene conformations in the amorphous region becomes indistinguishable from that in the crystalline regions. The latter result suggests that some correlations involving the properties of annealed poly(ethylene terephthalate) should be based on gauche-trans ratio rather than weight fraction of crystallinity.

The analysis of molecular motion in polymers, particularly those motions responsible for mechanical properties, has historically relied on dielectric and mechanical measurements.^{1,2} However, the assignment of low-temperature dielectric and mechanical loss peaks to specific molecular motions often requires extensive supplemental information from other measurements such as infrared, ^1H NMR, X-ray diffraction, and calorimetry. Even when reasonable assignments can be made, it is not always clear that the types of motions which occur at low temperatures are necessarily related to room-temperature molecular motions and mechanical properties.

We have shown previously that high-resolution carbon-13 NMR spectra can be obtained of solid glassy polymers³ and that measurement of relaxation parameters for the resolved resonances allows an unambiguous assignment of molecular motion in the mid-kilohertz frequency range.⁴⁻⁶

Furthermore, we have shown a correlation between these NMR relaxation parameters and the room-temperature impact strength for a variety of polymers.⁷ We report here the results of an analysis of the molecular motions at 26 °C in poly(ethylene terephthalate) (PET) as derived from carbon-13 rotating-frame relaxation measurements. We report also the effects of annealing on those molecular motions and the relationship between microscopic molecular motions and the transition from ductile to brittle mechanical behavior resulting from the annealing.

Experiments

Poly(ethylene terephthalate) (Goodyear Tire and Rubber Co., lot no. VFR 1625A) was vacuum-oven dried, melt pressed at 270 °C, and quenched in ice water to form either 0.3- or 3.2-mm films. These are referred to hereafter as thin and thick films, respectively. The films were clear, free from visible voids and defects, and

showed no crystallinity by X-ray diffraction. Biaxially oriented Mylar film 0.02-mm thick was obtained from E. I. du Pont de Nemours and Co.

All of the samples were stored at 22 °C and 40% relative humidity. Films were annealed at 61, 140 and 200 °C for varying times in an air bath and then quenched in ice water. Crystallinity of the PET samples was determined from density measurements and differential scanning calorimetry (DSC). Densities were determined according to ASTM 1505-60T in a hexane-carbon tetrachloride linear gradient. The crystallinity was calculated assuming a density of 1.333 g cm⁻³ for the amorphous region and 1.515 g cm⁻³ for the crystalline region.⁸ A Du Pont thermal analyzer 990 was used for the DSC measurements on approximately 5-mg samples with a heating rate of 10 °C/min under flowing nitrogen. The weight fraction of the crystalline region was calculated assuming the heat of fusion of fully crystalline PET to be 5.8 cal/mol.⁹ The mechanical properties of the quenched and annealed PET thin films were measured by a biaxial dart impact tester similar to that described by Larble and Supnik.¹⁰

Most of the carbon-13 NMR experiments were performed at 15.09 MHz with high-speed sample rotation at the magic-angle in a Beams-Andrews design hollow rotor. Details of the experimental conditions necessary to achieve high resolution from solids have been described elsewhere.^{3-7,11}

Cross-polarization spectra were obtained with single 1-ms contact times and matched H_1 's of 37 kHz. The carbon $T_{1\rho}$ relaxation time was obtained from a plot of the relative magnitude of the carbon magnetization remaining spin locked after the proton radio-frequency field was removed for varying times. The initial slope of the $T_{1\rho}$ curve (measured as described in footnote a, Table I) gave the average relaxation time, $\langle T_{1\rho}(C) \rangle$.

Proton $T_{1\rho}$'s and matched spin-lock cross-polarization 1-ms times, $T_{1S}(SL)$'s, were obtained from the carbon-13 NMR spectra as a function of carbon-proton contact time. The value of $T_{1\rho}(H)$ was given by the final slope of the magnetization vs. contact-time curve, while $T_{1S}(SL)$ was derived from the initial rise in polarization. The initial rate of nontransient polarization transfer from protons spin-locked in their dipolar field to carbons under an applied radio-frequency field was used to determine $\langle T_{1S}(ADRF) \rangle$.⁶ The latter measurements were obtained at 22.6 MHz on stationary samples with $H_1(C)$'s of 28, 37, and 44 kHz, respectively.

The homogeneous line width of the quenched thick PET films was determined from a spin-echo experiment. After an initial polarization with single 1-ms contacts at 37 kHz, the carbon radio-frequency field was turned off for a time τ , followed by a 180° refocusing pulse. The free induction decay was observed after a second time τ , where τ varied from 0.5 to 8 ms.

All measurements were made on samples which occupied approximately two-thirds the volume of the radio-frequency coil.

Results

Sample preparation and thermal history have pronounced effects on the observed PET chemical shifts and line shapes (Figure 1). Spectra are shown of PET which had been quenched (top left), annealed at 61 °C (bottom left), annealed at 140 °C (center), and annealed at 200 °C (top right). The spectrum of a biaxially oriented film with the transverse draw direction aligned with the magic angle is also shown (bottom right). The combination of dipolar decoupling and magic-angle spinning results in sufficiently high resolution to resolve the ethylene-, aromatic-, and carbonyl-carbon lines, which appear at 63, 133, and 165 ppm (δ_C), respectively.

The echo decay curves shown in Figure 2 indicate greater homogeneous line widths for the ethylene-carbon lines than for the aromatic- and carbonyl-carbon lines. Additional relaxation parameters for the ethylene-carbon lines of thick PET films are given in Table I. At a constant annealing temperature of 61 °C, increased annealing time generally results in increased $T_{1\rho}(C)$'s. For example, at a rotating-frame frequency of 37 kHz, $\langle T_{1\rho}(C) \rangle$ for the ethylene-carbon line increases from 3.5 to 6 ms after annealing a quenched sample for 350 h at 61 °C (Figure 3). Compa-

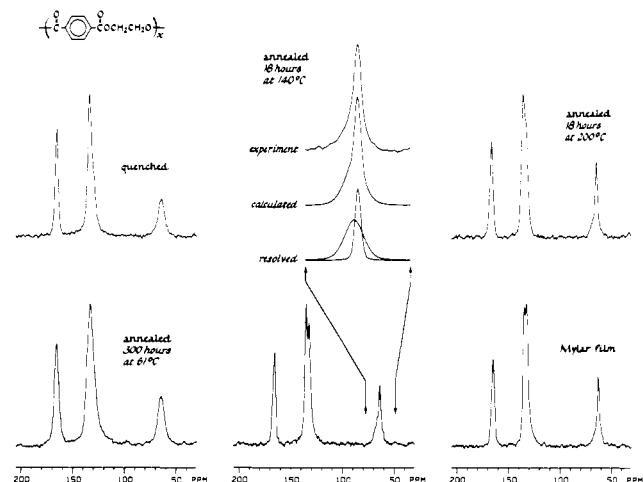


Figure 1. Cross-polarization magic-angle carbon-13 NMR spectra of methylene annealed, and biaxially oriented poly(ethylene terephthalate). The ethylene-, aryl-, and carbonyl-carbon resonances appear at 63, 133, and 165 ppm, respectively. An example of the deconvolution of the ethylene-carbon resonance into broad and narrow components is shown in the top, center section of the figure.

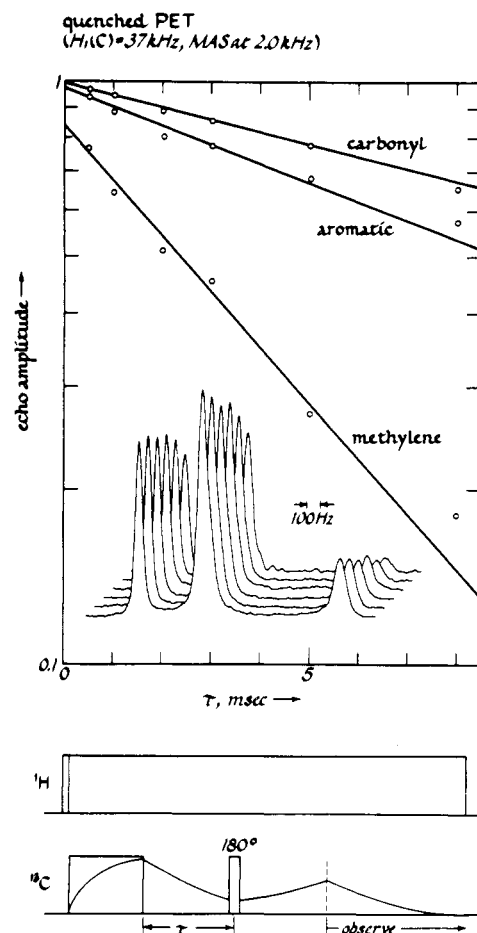


Figure 2. Cross-polarization magic-angle echo amplitudes for quenched poly(ethylene terephthalate). Slopes of the plotted lines yield homogeneous line widths of 35, 13, and 8 Hz for the ethylene-, aromatic-, and carbonyl-carbon resonances, respectively. The pulse sequence used to obtain these homogeneous line widths is illustrated in the bottom of the figure. The data were not influenced by minor attenuations of the echo amplitude which might arise from the interference of the single 180° pulse with the magic-angle averaging process, since the refocusing pulse was introduced only at even multiples of the rotor period.

table results were obtained for both thick and thin films (Tables I and II).

Table I
Relaxation Parameters for the Ethylene Carbons of
3-mm-Thick Films of
Poly(ethylene terephthalate) at 26 °C

annealing time at 61 °C, h	H_1 (C), kHz	$\langle T_{1\rho}(C) \rangle^a$, ms	$\langle T_{1S} \rangle^b$, ms	$T_{1\rho}(H)$, ms
0	28	2.1	100	2.9
	37	3.5	>100	
	44	7.0	>100	
30	28	2.1	85	3.7
	37	4.9	>100	
	44	9.8	>100	
350	28	2.7	70	3.9
	37	6.0	>100	
	44	10.0	>100	

^a Sample spinning at 2.1 kHz at the magic angle; average value is the least-squares straight-line fit of the relaxation data collected from 0.300 to 0.800 ms after removal of the 1H radio-frequency field. Accuracy estimated at $\pm 10\%$. Carbon polarization prepared by a 1-ms matched spin-lock transfer. ^b Stationary sample; average value obtained from $(dS/dt)_{t=0}$, using ADRF polarization transfer from 0.300 to 0.800 ms after initial contact.

Table II
 $\langle T_{1\rho}(C) \rangle$ for Annealed
Poly(ethylene terephthalate) Thin Films^{a,b}

annealing conditions	density (ρ)	% crys- tal- linity (w_c from ρ)	$\langle T_{1\rho}(C) \rangle$, ms		
			ethyl- ene	aro- ma- tics	car- bonyl
quenched	1.337	2	3.5	18	27
annealed at 61 °C (30 h)	1.339	3	5.1	15	34
annealed at 61 °C (276 h)	1.340	3	5.7	9	44
annealed at 140 °C (18 h)	1.377	34	16	20	120
annealed at 200 °C (18 h)	1.400	37	21	18	110
Mylar		50 ^c	18	23	130

^a Relaxation times measured at 15.09 MHz on 0.3-mm samples spinning at 2.0 kHz at the magic angle with carbon and proton H_1 's of 37 kHz. Sample temperature was 26 °C. Method of measuring $\langle T_{1\rho}(C) \rangle$ was as described in footnote a, Table I. ^b Mylar film (0.02 mm) used as supplied from Du Pont. ^c Du Pont estimate based on X-ray diffraction.

The $\langle T_{1\rho}(C) \rangle$'s for the ethylene-carbon lines have a stronger dependence on the rotating-frame frequency than do the $\langle T_{1\rho}(C) \rangle$'s for the aromatic-carbon lines. The ethylene-carbon $\langle T_{1\rho}(C) \rangle$'s measured at H_1 's of 28, 37, and 44 kHz have about a square-law dependence on $H_1(C)$ (Table I). By contrast, aromatic-carbon $\langle T_{1\rho}(C) \rangle$'s of 8, 12, and 15 ms were observed for the same H_1 's (for the thick-film sample annealed at 61 °C for 30 h), a dependence somewhat less than square law.

Proton-carbon matched spin-lock cross-polarization transfer times, $T_{1S}(SL)$, for the ethylene carbons were 29, 31, and 28 μ s, respectively, for 0, 30, and 350 h of annealing at 61 °C. The average cross-polarization transfer times for the sum of the protonated and nonprotonated aromatic-carbon lines were 161, 113, and 90 μ s for samples annealed 0, 30, and 350 h, respectively.

Annealing thin PET films results in an increase in the $\langle T_{1\rho}(C) \rangle$ of the ethylene- and carbonyl-carbon lines but a decrease in the $\langle T_{1\rho}(C) \rangle$ for the aromatic-carbon line, until the onset of crystallinity (Table II). Annealing PET films above T_g not only causes significant changes in the relaxation parameters but also alters the line shape (Figure

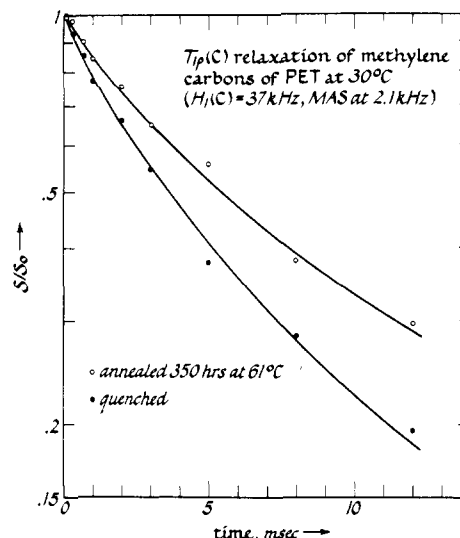


Figure 3. Carbon-13 rotating-frame relaxation data for the methylene carbons of poly(ethylene terephthalate) showing the dispersion which results from a distribution of relaxation times. The average relaxation time, represented by the initial slope (see text) of the relaxation curve, is 3.5 ms for quenched (open circles) and 6.0 ms for annealed (closed circles) poly(ethylene terephthalate). The annealing was performed at 61 °C for 350 h. The samples are described in Table I.

1). The ethylene-carbon line assumes an asymmetric shape when annealed above T_g , suggesting contributions from both broad and narrow components. With the aid of computer analysis, these two components of the ethylene-carbon resonance can be resolved for samples where $T_a = 140$ and 200 °C (see, for example, Figure 1, top center). The narrow component is shifted upfield about 1 ppm relative to the broad component. From such resolved curves, the broad and narrow components of the PET sample with $T_a = 140$ °C have $\langle T_{1\rho}(C) \rangle$'s of 6.5 and 26 ms, respectively. Deconvolution of the ethylene-carbon resonance for the sample annealed at 200 °C yields relaxation times of 10 and 27 ms for broad and narrow components, respectively. Included in Table II for comparison are the results obtained with a biaxially oriented Mylar film which is reported to have approximately 50% crystallinity.¹²

The density and calculated weight fraction crystallinity, w_c , for the annealed thin films are included in Table II. Differential scanning calorimetry measurements for the film annealed at 140 °C gave two endotherms ($T_{max} = 155.0$ and 256.7 °C) with a combined $\Delta H = 10.52 \pm 0.03$ cal/g. Annealing at 200 °C also produces a film with two endotherms ($T_{max} = 226.5$ and 258.9 °C) with $\Delta H = 11.69 \pm 0.19$ cal/g.

Impact strengths of PET thin films determined by the falling-dart test are presented in Table III. The near-linear relationship between film thickness and failure energy has been used in reporting the results as an average of 8–12 specimens ranging in thickness from 0.2 to 0.3 mm.

Discussion

Origin of Line Widths. The carbon-13 NMR spectrum of quenched PET (Figure 1, upper left) has three resonances arising from the carbonyl, aryl, and ethylene carbons, in order of increasing field, from left to right. These three lines are fairly broad (with widths of 60, 100, and 90 Hz, respectively), even in the presence of dipolar decoupling and magic-angle spinning. The line widths observed can be due either to heterogeneous broadening factors such as distributions of isotropic chemical shifts¹³ or to homogeneous broadening factors arising from mo-

Table III
Dynamic Mechanical Properties of
Poly(ethylene terephthalate) Films from
Biaxial Dart Impact Test

annealing conditions	strength, ^{a, b} N	failure energy, mJ
quenched	196 ± 7	340 ± 6
annealed at 61 °C (24 h)	120 ± 9	42 ± 6
annealed at 61 °C (115 h)	121 ± 9	42 ± 6

^a Film thicknesses between 0.2 and 0.3 mm were used; reported results are normalized to 0.4-mm thickness.

^b Strength is determined by the output of a quartz-crystal transducer mounted beneath a 6.5-mm-diameter dart. The 25-mm-diameter film sample, clamped over a 16-mm-diameter hole in the falling plate, impacts the dart at a rate of 365 cm/s.

lecular motion described by an effective autocorrelation frequency comparable to the decoupling field.

We do not expect large chemical shift differences for the various ethylene conformations since interactions with γ substituents should be small.¹⁴ In addition, over the period from 0.5 to 8 ms the echo amplitudes (Figure 2) decay at about the same rate as $T_{1\rho}(C)$ (Figure 3). That is, the observed ethylene-carbon line width is comparable to $\langle T_{1\rho}(C) \rangle^{-1}$. This indicates that much of the broadening arises from the motional shortening¹⁵ of the dipolar-decoupled carbon T_2 . Consistent with this interpretation we observe a reduced ethylene-carbon line width for biaxially oriented¹⁶ PET (Figure 1, lower right). We suspect that the predominantly trans-ethylene conformations¹⁷ in Mylar not only produce an isotropic upfield shift of about 1 ppm but also reduce molecular motions, increasing $T_{1\rho}(C)$ and decreasing the line width.

Homogeneous line widths are less and $T_{1\rho}(C)$'s are greater for the aromatic and carbonyl carbons of PET than for the ethylene carbons (Table II and Figure 2). This is to be expected since the broadening depends on the strength of the fluctuating dipolar field, and dipolar interactions experienced by the ethylene carbons are stronger than for the aromatic and carbonyl carbons. Nevertheless, the observed aromatic- and carbonyl-carbon line widths are still consistent with substantial (but not complete) homogeneous broadening from molecular motion with frequency components comparable to the decoupling field. Rotation of the phenyl ring about its C-1, C-4 axis as proposed by Tonelli¹⁸ and others¹⁹ could lead to considerably greater homogeneous line widths for the protonated carbons than for the nonprotonated C-1 and C-4 carbons. The asymmetric line shape in the aromatic region of the spectrum of quenched PET (Figure 1, upper left) could result from the overlap of a relatively narrow downfield line, arising from the two nonprotonated carbons, and a broader line, shifted upfield,¹³ for the four protonated aromatic carbons.

$\langle T_{1\rho}(C) \rangle$ as a Measure of Molecular Motion. The loss of carbon magnetization from the rotating frame can occur through either spin-lattice or spin-spin processes. Spin-lattice relaxation arises from the modulation of internuclear dipolar interactions by molecular motion at the rotating-frame Larmor frequency (low-to-mid-kilohertz range). Spin-spin relaxation results from strong, static ^1H - ^1H interactions and proton spin flips which produce a broad dipolar fluctuation spectrum with substantial spectral density at the carbon rotating-frame Larmor frequency.^{20,21} Mutual spin flips can then occur from spin-locked carbons to protons, resulting in a loss of carbon polarization characterized by a spin-spin time constant $T_{\text{IS}}(\text{ADRF})$.⁶

In the absence of any spin-lattice process, $\langle T_{\text{IS}}(\text{ADRF}) \rangle$ is equal to $\langle T_{1\rho}(C) \rangle$. For quenched PET samples and for samples annealed below T_g , $\langle T_{\text{IS}}(\text{ADRF}) \rangle$ is more than an order of magnitude larger than $\langle T_{1\rho}(C) \rangle$ for all H_1 's examined here (Table I). Thus, $\langle T_{1\rho}(C) \rangle$ for the ethylene carbons of amorphous PET is determined by molecular motion. The weak H_1 dependence of $\langle T_{1\rho}(C) \rangle$ suggests this is also true for the aromatic carbons.

Carbon rotating-frame relaxation in crystalline regions of PET, and other crystalline polymers for that matter, may be dominated by spin-spin processes.⁴ We previously reported⁴ a value of 54 ms for the $\langle T_{\text{IS}}(\text{ADRF}) \rangle$ for the ethylene carbons of Mylar at 37 kHz. Assuming 50% crystallinity for our sample of Mylar, we can estimate the $\langle T_{\text{IS}}(\text{ADRF}) \rangle$ in the crystalline regions of the sample by

$$\frac{1}{\langle T_{\text{IS}}(\text{ADRF}) \rangle_{\text{Mylar}}} = \frac{0.5}{\langle T_{\text{IS}}(\text{ADRF}) \rangle_{\text{cryst}}} + \frac{0.5}{\langle T_{\text{IS}}(\text{ADRF}) \rangle_{\text{amorph}}}$$

From Table I $\langle T_{\text{IS}}(\text{ADRF}) \rangle_{\text{amorph}}$ is greater than 100 ms so that by the above equation $\langle T_{\text{IS}}(\text{ADRF}) \rangle_{\text{cryst}}$ is estimated to be about 30 ms. From the deconvolution procedures described earlier, the $\langle T_{1\rho}(C) \rangle$'s for the ethylene carbons in the crystalline regions of Mylar and of annealed un-oriented PET are found to be 26–27 ms. Thus, $\langle T_{1\rho}(C) \rangle \sim \langle T_{\text{IS}}(\text{ADRF}) \rangle$, relaxation in crystalline PET is spin-spin dominated, and no information about molecular motion is available.

Frequency of Molecular Motion in PET. The presence of motional broadening in the ^{13}C NMR spectrum of quenched PET indicates the presence of molecular motion with components described by correlation frequencies comparable to the decoupling field ($H_1 = 37$ kHz) at 26 °C. This conclusion is in general agreement with those based on other experiments. For example, Ward²² concluded from his study of PET with proton nuclear magnetic resonance that the ethylene carbons undergo considerable reorientation at frequencies greater than 10^5 Hz and that some phenyl reorientation also occurs at these frequencies. On the basis of the time-temperature superposition principle, dynamic mechanical^{1,2,23,24} and dielectric loss²⁵ spectra have been generally interpreted as indicating relatively high-frequency motions for the ethylene-carbon reorientation (γ relaxation), and somewhat lower frequencies for phenyl and carbonyl motion (β relaxation) at room temperature. Williams and Flory²⁶ and Tonelli¹⁹ have presented theoretical arguments for the treatment of the phenyl residue as a free rotor, so that restricted, essentially independent torsional oscillations in the solid state are not completely unreasonable.

As we have already described, the spin-lattice contribution to $T_{1\rho}(C)$ is sensitive to rotational segmental motions of the polymer chain in the frequency range determined by the carbon H_1 . A qualitative interpretation⁷ of the Bloembergen-Pound-Purcell²⁷ theory of magnetic relaxation in terms of the rotating-frame rare-spin experiment predicts that the $T_{1\rho}(C)$ should vary as $(H_1(C))^2$ for relaxation induced by motions whose frequencies are less than $H_1(C)$. Relaxation due to motions which have frequency components much greater than $H_1(C)$ have little or no dependence on the rotating-frame frequency. By this argument, the rotating-frame frequency dependence of the ethylene-carbon $\langle T_{1\rho}(C) \rangle$'s (Table I) of quenched and annealed ($T_a < T_g$) PET is consistent (within experimental error) with relaxation being dominated by molecular motion in the low-to-mid-kilohertz frequency range. Phenyl-carbon $\langle T_{1\rho}(C) \rangle$'s increase only by a factor of 2 for

a change of H_1 's from 28 to 44 kHz (see Results), suggesting that some independent phenyl reorientation may occur at higher average frequencies than ethylene-carbon motion. Both ethylene- and phenyl-carbon $T_{1\rho}$ relaxation plots show the presence of multiple relaxation times and so distributions of amplitudes and frequencies of motions.

Effects of Annealing on Molecular Motion. 1. **Annealing below T_g .** Annealing has a profound effect on the physical properties of PET.^{28,32} Annealing below T_g rapidly results in embrittlement, indicated by failure in tensile and impact strength tests. This is true even though the low-temperature region of the dynamic mechanical loss spectrum of annealed PET is indistinguishable from that of quenched PET.³³ (Yip and Williams³⁵ have summarized most of the recent mechanical data in their study of relaxations in polyesters related to PET.)

The $\langle T_{1\rho}(C) \rangle$ data reported in Table II indicate the sensitivity of rotating-frame relaxation to thermal history for thin PET films. Annealing at 61 °C ($T_a < T_g$) leads to an increase in the $\langle T_{1\rho}(C) \rangle$ for the ethylene and carbonyl carbons and a decrease in that for the aryl carbons. Now, we might expect lower amplitude motions and longer $\langle T_{1\rho}(C) \rangle$'s for ethylene carbons in trans conformations than for those in gauche conformations. However, annealing below T_g does not provide sufficient energy to allow for conversion between these two conformations.³⁴ Rather, we believe the decrease in the ethylene-carbon $\langle T_{1\rho}(C) \rangle$ reflects a decrease in the amplitude (or frequency) of the cooperative ethylene-group motion (lowering the spectral density at the carbon rotating-frame frequency) by elimination of nonequilibrium interchain configurations and free volume trapped by the quenching process.³⁶

The $\langle T_{1\rho}(C) \rangle$'s of ethylene and carbonyl carbons increase by the same ratio when thin films of PET are annealed below T_g (Table II). This result suggests that the carbonyl carbons are being relaxed by motions of the ethylene protons. (The larger values of the carbonyl $\langle T_{1\rho}(C) \rangle$ compared to that of the ethylene carbons reflects the strong dependence on the internuclear distance for dipolar interactions.) We interpret the parallel behavior of the ethylene- and carbonyl-carbon $\langle T_{1\rho}(C) \rangle$'s as an indication that independent motion of the carbonyl group does not change significantly when the sample is annealed below T_g . This interpretation is consistent with dynamic mechanical measurements which show no change in the low-temperature loss for quenched films and for films annealed at 65 °C.³³ (Loss in the temperature region of -100 to -60 °C is generally regarded as due to COO motion.³⁵)

The $\langle T_{1\rho}(C) \rangle$ for the sum of the protonated and non-protonated aryl carbons is about 3 times longer than for the ethylene carbons in quenched PET, roughly consistent with the number of directly bonded protons and equal average angular excursions for methylene and aromatic carbon-proton internuclear vectors. These excursions represent rotational reorientations within conformations. The decrease in aromatic-carbon $\langle T_{1\rho}(C) \rangle$ with annealing at 61 °C (Table II) implies that phenyl motion, which has components of motion at higher frequencies than $H_1(C)$ in the quenched state, is either reduced in frequency or increased in amplitude. On the basis of the present experiments we cannot choose between the two possibilities. The former seems less likely, however, in view of reasonable arguments that the development of precrystalline order leads to loss of phenyl-carbonyl coplanarity and hence a loss of cooperative relaxation¹⁷ but an increase in independent or internal relaxation.

2. **Annealing above T_g .** Annealing above T_g causes densification and formation of crystalline domains. Pro-

nounced changes in the high-temperature region of the mechanical loss spectrum are observed, as well as modest changes in the low-temperature region, the latter including a slight decrease in the intensity and temperature of the adsorption maxima.³⁴ Annealing above T_g also results in large changes in the observed $\langle T_{1\rho}(C) \rangle$'s. After annealing at 140 °C the ethylene-carbon line shape shows structure which can be resolved into broad and narrow components (Figure 1, top center). These components have $\langle T_{1\rho}(C) \rangle$'s of 6.5 and 26 ms, respectively. On the basis of relative areas, the narrow component comprises 37% of the total ethylene-carbon intensity. The high-field narrow component arises from the trans-ethylene conformations, including those in the amorphous region. The latter conclusion is supported by two arguments: (1) the NMR experiment is sensitive to molecular environments which extend only a few repeat units and hence detects ordered regions that are much smaller than those usually described as crystalline, and (2) the percentage of ethylene carbons contributing to the narrow component is greater than the percentage crystallinity determined from density measurements. Infrared studies support the notion that the percentage of trans-ethylene conformations in heat-set PET films is generally greater than the percent crystallinity.¹⁶

The value of 6.5 ms for the $\langle T_{1\rho}(C) \rangle$ for the broad component of the ethylene-carbon region represents a continuation of the trend of increasing $T_{1\rho}$ with increasing annealing that was observed with samples annealed below T_g (Table I). This result is possibly explained by the fact that, in addition to relieving strained conformations and reducing free volume, annealing above T_g results in formation of small crystallites which further inhibit motion in the amorphous region. On the basis of shifts in high-temperature loss peaks observed from annealed PET samples of varying crystallinity, Illers and Breuer³⁴ suggested that at low-to-medium crystallinities there may be many small crystallites which act as cross-links to inhibit cooperative segmental motion in the amorphous phase. At high crystallinities, they would argue the individual crystallites are larger and the ratio of amorphous volume to the number of crystals increases. This leads to speculation of increased segmental motion in the amorphous phase. Nevertheless, our data indicate a decrease in molecular motion of the gauche-ethylene conformations of the amorphous region even after annealing at 200 °C ($\langle T_{1\rho}(C) \rangle_{\text{broad}} = 10.5$ ms) where large crystallites might be expected. We conclude that precrystalline ordering has more to do with inhibition of motion than the more macroscopic effects of the large crystallites themselves.

Just as with annealing below T_g , $\langle T_{1\rho}(C) \rangle$'s for the carbonyl carbons of PET films annealed above T_g lengthen in proportion with the ethylene-carbon $\langle T_{1\rho}(C) \rangle$'s, suggesting that relaxation is provided by motion of the ethylene protons. The increased value of the aryl-carbon $\langle T_{1\rho}(C) \rangle$ and changing line shape³⁷ are also a result of increasing crystallinity. However, a quantitative interpretation of the aryl- and carbonyl-carbon $\langle T_{1\rho}(C) \rangle$'s is unwarranted, since their line shapes do not allow a resolution of components from different regions of the polymer as was possible for the ethylene-carbon line.

Molecular Motion and Mechanical Properties of PET. We have previously demonstrated a correlation between mechanical properties of nominally homogeneous glassy polymers and NMR relaxation parameters.^{5,7} In that correlation we pointed out that a short main-chain $T_{1\rho}(C)$ often corresponds to high impact strengths since the former indicates main-chain motions fast enough to

lead to plastic flow, thereby dissipating impact energy as heat without stress concentration, crack formation, and brittle failure.⁴ Consistent with this correlation, the ethylene-carbon $\langle T_{1\rho}(C) \rangle$'s of PET increase by just a little less than a factor of 2 when quenched films are annealed at 61 °C for about 30 h. This is true despite the use of a far more conservative procedure for measuring $\langle T_{1\rho}(C) \rangle$ than employed previously.⁴ These changes in $\langle T_{1\rho}(C) \rangle$ are accompanied by a decrease in the impact strength (Table III).

Embrittlement has been reported in PET films annealed as low as 51 °C for 90 min.³³ On the basis of the relationship of annealing time and temperature to the transition from ductile-to-brittle failure, Mininni et al.³³ proposed that this transition was due to the elimination of an extremely small increment of trapped free volume. Indeed, little densification occurs under these annealing conditions.

We suggest that ductile behavior in quenched PET arises from cooperative high-frequency components of motion associated with trapped, nonequilibrium ethylene configuration.³⁶ These motions are the precursors to plastic flow. Annealing removes these motions resulting in either slow cooperative motions or fast but localized (independent, noncooperative) phenyl-group motions, neither of which is well suited to initiating plastic flow. Loss of just a few high-frequency cooperative motions is apparently sufficient to precipitate a change in failure mode from ductile to brittle. After the ductile–brittle failure transition or threshold has been reached, the ethylene-carbon $\langle T_{1\rho}(C) \rangle$ continues to increase with additional annealing but with no further decrease in impact strength observed (Table III). In this regime, brittle failure is now correlated with volume or dilational effects, including internal flaws, inclusions, surface defects, and sample thickness, all of which are effects unrelated to microscopic molecular motion.⁵

References and Notes

- (1) T. Murayama, "Dynamic Mechanical Analysis of Polymeric Materials", Elsevier, New York, 1978.
- (2) R. F. Boyer in "Polymeric Materials: Relationship between Structure and Mechanical Properties", E. Baer and S. V. Radcliffe, Eds., American Society for Metals, Metals Park, OH, 1974, Chapter 6, pp 227–368.
- (3) J. Schaefer, E. O. Stejskal, and R. Buchdahl, *Macromolecules*, **8**, 291 (1975).
- (4) J. Schaefer, E. O. Stejskal, T. R. Steger, M. D. Sefcik, and R. A. McKay, *Macromolecules*, accompanying paper in this issue.
- (5) T. R. Steger, J. Schaefer, E. O. Stejskal, and R. A. McKay, *Macromolecules*, preceding paper in this issue.
- (6) E. O. Stejskal, J. Schaefer, and T. R. Steger, *Faraday Symp. Chem. Soc.*, **13**, 56 (1979).
- (7) J. Schaefer, E. O. Stejskal, and R. Buchdahl, *Macromolecules*, **10**, 384 (1977).
- (8) S. Fakirov, E. W. Fischer, and G. P. Schmidt, *Makromol. Chem.*, **176**, 2459 (1975).
- (9) B. Wunderlich, "Macromolecular Physics", Vol. 1, Academic Press, New York, 1973, p 389.
- (10) R. C. Larble and R. H. Supnik, "High Speed Testing", Vol. IV, A. G. Dietz and F. R. Eirich, Eds., Interscience, New York, 1964, p 283.
- (11) J. Schaefer and E. O. Stejskal, *Top. Carbon-13 NMR Spectrosc.*, **3**, 302–6 (1979).
- (12) C. J. Heffelfinger, private communication.
- (13) R. A. Komoroski, *J. Polym. Sci., Polym. Phys. Ed.*, **17**, 45 (1979).
- (14) A. E. Tonelli, *Macromolecules*, **12**, 255 (1979).
- (15) A. N. Garroway, W. B. Muniz, and H. A. Resing, *ACS Symp. Ser.*, No. 103, 67 (1979).
- (16) C. J. Heffelfinger and P. G. Schmidt, *J. Appl. Polym. Sci.*, **9**, 2661 (1965).
- (17) P. G. Schmidt, *J. Polym. Sci., Part A*, 1271 (1963).
- (18) A. E. Tonelli, *J. Polym. Sci., Polym. Lett. Ed.*, **11**, 441 (1973).
- (19) E. Sacher, *J. Macromol. Sci., Phys.*, **B5**, 739 (1971).
- (20) A. Pines, M. G. Gibby, and J. S. Waugh, *J. Chem. Phys.*, **59**, 569 (1973).
- (21) D. A. McArthur, E. L. Hahn, and R. E. Walstadt, *Phys. Rev.*, **188**, 609 (1969).
- (22) I. M. Ward, *Trans. Faraday Soc.*, **56**, 648 (1960).
- (23) C. D. Armeniades and E. Baer, *J. Polym. Sci., Part A-2*, **9**, 1345 (1971).
- (24) V. Frosini and A. E. Woodward, *J. Macromol. Sci., Phys.*, **B3**, 91 (1969).
- (25) E. Sacher, *J. Macromol. Sci., Phys.*, **B15**, 257 (1978).
- (26) A. D. Williams and P. J. Flory, *J. Polym. Sci., Part A-2*, **5**, 417 (1967).
- (27) N. Bloembergen, E. M. Purcell, and R. V. Pound, *Phys. Rev.*, **74**, 679 (1948).
- (28) M. Takayanagi, M. Yoshino, and S. Minami, *J. Polym. Sci.*, **61**, S7 (1962).
- (29) E. Ito and T. Hatakeyama, *J. Polym. Phys.*, **12**, 1477 (1974).
- (30) E. W. Fischer and S. Fakirov, *J. Mater. Sci.*, **11**, 1041 (1976).
- (31) S. Fakirov, E. W. Fischer, R. Hoffmann, and G. F. Schmidt, *Polymer*, **18**, 1121 (1977).
- (32) J. H. Dumbleton and T. Murayama, *Kolloid-Z. Z. Polym.*, **220**, 41 (1967).
- (33) R. M. Mininni, R. S. Moore, J. R. Flick, and S. E. B. Petrie, *J. Macromol. Sci., Phys.*, **B8**, 343 (1973).
- (34) K. H. Illers and H. Breuer, *J. Colloid Sci.*, **18**, 1 (1963).
- (35) H. K. Yip and H. L. Williams, *J. Appl. Polym. Sci.*, **20**, 1217 (1976).
- (36) I. H. Hall, *Polymer*, **13**, 69 (1972).
- (37) C. A. Fyfe, J. R. Lyster, W. Volksen, and C. S. Yannoni, *Macromolecules*, **12**, 757 (1979).